Vibration control of base-isolated structures using mixed H_2/H_∞ output-feedback control

H R Karimi[1]*, **M Zapateiro**[2], and **N Luo**[2]
[1]Faculty of Technology and Science, University of Agder, Grimstad, Norway
[2]Institute of Informatics and Applications, University of Girona, Girona, Spain

The manuscript was received on 27 December 2008 and was accepted after revision for publication on 18 May 2009.

DOI: 10.1243/09596518JSCE730

Abstract: A mixed H_2/H_∞ output-feedback control design methodology for vibration reduction of base-isolated building structures modelled in the form of second-order linear systems is presented. Sufficient conditions for the design of a desired control are given in terms of linear matrix inequalities. A controller that guarantees asymptotic stability and a mixed H_2/H_∞ performance for the closed-loop system of the structure is developed, based on a Lyapunov function. The performance of the controller is evaluated by means of simulations in MATLAB/Simulink.

Keywords: vibration reduction, mixed H_2/H_∞ output-feedback, LMI

1 INTRODUCTION

The protection of civil engineering structures has always been a major concern especially when these structures are built in places prone to hazardous weather conditions (e.g. hurricanes, tsunamis), zones of intense seismic activity, or when the structure is subjected to heavy loadings (e.g. heavy traffic on a bridge). If a structure is not well protected against these phenomena, they can suffer severe damage and, as a consequence, produce personal injury or death, as during the earthquakes in Mexico City (1985), Kobe (1995), northwestern Turkey (1999), those that struck southern Asia in 2004 followed by the tsunamis, or more recently in China (2008).

In order to make structures more resistant to these phenomena, passive and active dampers have been proposed. Passive dampers alleviate the energy dissipation of the main structure by absorbing part of the input energy, without the need of external power sources. However, once installed, they are not adaptable to changing loading conditions [**1**]. Active dampers, on the other hand, can respond to variations in the loading conditions and structural dynamics but require large power sources and additional hardware such as sensors and digital signal processors (DSPs) to operate. Active dampers can also inject energy to the structure and may destabilize it in a bounded-input bounded-output sense [**2**]. Semi-active devices provide an effective solution to overcome the disadvantages of passive and active dampers [**3**]. They have been shown to perform significantly better than passive devices, and as well as active devices, without requiring large power sources, thus allowing for battery operation [**4**]. The main characteristic of semi-active devices is the rapid adaptability of their dynamic properties in real time but without injecting any energy into the system. Among diverse semi-active devices, magnetorheological (MR) fluid dampers are the most attractive and useful ones. MR dampers can generate a high yield strength, have low production costs, require low power, and have a fast response and small size. However, they are characterized by a complex non-linear dynamics (typically hysteresis) which makes mathematical treatment challenging, especially in the modelling and identification of the hysteretic dynamics and the development of control laws for its implementation through MR dampers for vibration mitigation purposes. Recently, semi-active H_∞ control of a vehicle suspension with an MR damper was studied [**5**]. More recently, in reference

*Corresponding author: Department of Engineering, Faculty of Engineering and Science, University of Agder, Serviceboks 509, Grimstad 4898, Norway.
email: hamid.r.karimi@uia.no

[**6**], a computational algorithm was presented for the modelling and identification of MR dampers by using wavelet systems to handle the non-linear terms. By taking into account the Haar wavelets, the properties of an integral operational matrix and product operational matrix were introduced and then utilized to estimate the MR damper parameters by considering only algebraic equations instead of the differential equations of the dynamical system.

On the other hand, second-order systems capture the dynamic behaviour of many natural phenomena, and have found applications in many fields, such as vibration and structural analysis, spacecraft control, electrical networks, and robotics control, and hence have attracted considerable attention (see, for instance, references [**7**] to [**10**]). In the literature, some seminal works have been reported on the design of linear quadratic regulator (LQR) control [**11–13**], sliding mode control [**14**], H_2 control [**15**], H_∞ control [**16**, **17**], guaranteed-cost control [**18**, **19**], and multiobjective control [**20–24**] for second-order vibration systems.

In recent years, considerable attention has been paid to systematic applications of semi-active linear control algorithms for vibration control of building structures subject to natural hazards, e.g. earthquakes and strong winds; see, for instance, reference [**25**] and the references therein. A number of control techniques have been developed for vibration control of structures equipped with MR dampers. The clipped optimal control approach [**26**] was one of the first controllers developed for this class of systems. An optimal controller is designed to estimate the force that mitigates the vibrations in the structure, and the control signal takes only two values according to an algorithm, in which the MR damper dynamics are ignored. Control techniques based on Lyapunov's stability theory have been proposed and successfully tested in structures such as buildings, bridges, and car suspension systems [**27–32**]. The general control objective is achieved through the choice of control inputs that make the Lyapunov function derivative as negative as possible and consequently obtain the maximum energy dissipation. Other control methods have also been proposed such as bang-bang control [**27**, **33**, **34**], sliding mode control [**31**, **35**, **36**], backstepping control [**37**, **38**], and intelligent control such as fuzzy logic control [**39**] and neuro fuzzy control [**40**]. More recently [**41**], a neural network backstepping controller for a class of semi-active vehicle suspension systems equipped with MR dampers was presented. However, how to analyse and synthesize dynamic vibrational structures is a challenging problem of recurring interest because a building structure with MR dampers is a non-linear time-varying system, not a linear time-invariant one. This motivates the present study.

In this paper, the problem of vibration reduction in a base-isolated building structure is dealt with by using mixed H_2/H_∞ output-feedback control. Sufficient conditions are established such that the resulting closed-loop system is asymptotically stable and satisfies a prescribed mixed H_2/H_∞ performance. The proposed method provides a convex problem such that the control gain can be found from the linear matrix inequality (LMI) formulations based on a Lyapunov function. Finally, simulation results are given to illustrate the usefulness of the proposed control methodology.

The rest of this paper is organized as follows. Section 2 describes the system under consideration, and the problem formulation and definitions are stated in section 3. Section 4 includes the main results of the paper, that is, sufficient conditions for mixed H_2/H_∞ output-feedback control design methodology. Section 5 provides numerical results, and Section 6 concludes the paper.

Notation

The superscript 'T' stands for matrix transposition; $\Re^n$ denotes the n-dimensional Euclidean space; $\Re^{n\times m}$ is the set of all real m by n matrices. $\|.\|$ refers to the Euclidean vector norm or the induced matrix 2-norm. The L_∞ signal norm $\|\boldsymbol{v}(t)\|_\infty$ measures the maximum amplitude of the components v_i of a signal vector $\boldsymbol{v}$ over time t, i.e. $\|\boldsymbol{v}(t)\|_\infty := \sup_t \max_i |v_i(t)|$. Also, col$\{\cdots\}$ and diag$\{\cdots\}$ represent, respectively, a column vector and a block diagonal matrix, and the operator sym$(\mathbf{A})$ represents $\mathbf{A}+\mathbf{A}^{\mathrm{T}}$. The notation $\mathbf{P}>0$ means that $\mathbf{P}$ is real symmetric and positive definite; the symbol $*$ denotes the elements below the main diagonal of a symmetric block matrix and $\sigma_{\max}[.]$ denotes the largest singular value of [.]. In addition, $L_2[0, \infty)$ is adopted for the space of all functions $f: \Re \rightarrow \Re$ which are Lebesque integrable in the square over $[0, \infty)$, with the standard norm $\|.\|_2$.

2 SYSTEM DESCRIPTION

Consider a seismically excited base-isolated structure as shown in Fig. 1. The system dynamics can be divided into two subsystems, namely, the main structure (S_{r}) and the base (S_{c}) [**14**]

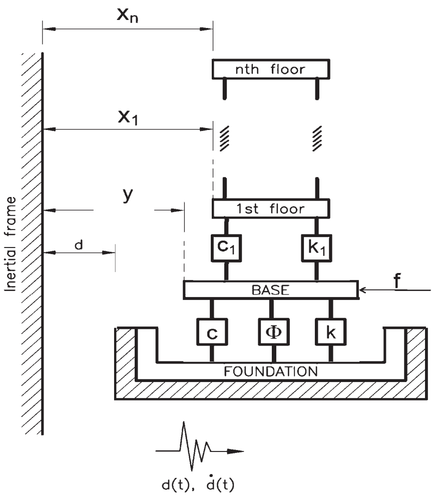

Fig. 1 Schematic of a base-isolated structure

$$S_r\text{: } \mathbf{M}\ddot{\boldsymbol{X}}(t)+\mathbf{C}\dot{\boldsymbol{X}}(t)+\mathbf{K}\boldsymbol{X}(t) = \left[c_1, \underbrace{0, \cdots, 0}_{n-1}\right]^{\mathrm{T}} \dot{y}(t) + \left[k_1, \underbrace{0, \cdots, 0}_{n-1}\right]^{\mathrm{T}} y(t) \tag{1a}$$

$$S_c\text{: } m\ddot{y}(t)+c\dot{y}(t)+ky(t)+f_{\mathrm{bf}}(t)=f_{\mathrm{g}}(t)+f(t) \tag{1b}$$

$$f_{\mathrm{bf}}(t)=c_1(\dot{y}(t)-\dot{x}_1(t))+k_1(y(t)-x_1(t)) \tag{1c}$$

$$f_{\mathrm{g}}(t)=-c\dot{d}(t)-k\,d(t)+\Phi\Big(\dot{y}(t),\dot{d}(t)\Big) \tag{1d}$$

$$\Phi\Big(\dot{y}(t),\dot{d}(t)\Big)=-\operatorname{sgn}\Big(\dot{y}(t)-\dot{d}(t)\Big) \times\Big(\mu_{\max}-\Delta\mu\,\mathrm{e}^{-\nu|\dot{y}(t)-\dot{d}(t)|}\Big)Q \tag{1e}$$

where $\boldsymbol{X}=[x_1, x_2, \ldots, x_n]^{\mathrm{T}}\in\Re^n$ is the horizontal absolute floor displacement vector, $y(t)\in\Re$ is the horizontal absolute base displacement, $d(t)$ and $\dot{d}(t)$ are the seismic excitation displacement and velocity, and $f(t)$ is the active control force applied to the base level. Equation (1c) accounts for the dynamic coupling between the base and the main structure. Equation (1d) describes the forces introduced by the seismic excitation and the base isolation. Equation (1e) describes the dynamics of a frictional base isolator, where $\mu_{\max}$ is the friction coefficient for high sliding velocity, $\Delta\mu$ is the difference between $\mu_{\max}$ and the friction coefficient for low sliding velocity, ν is a constant, and Q is the force normal to the friction surface. Parameters m, c, and k are the mass, damping coefficient, and stiffness of the base, while matrices **M**, **C**, and **K** are those of the main structure as follows

$$\mathbf{M}=\operatorname{diag}\{m_1, m_2, \cdots, m_n\} \tag{1f}$$

$$\mathbf{C}=\begin{bmatrix} c_1+c_2 & -c_2 & \cdots & 0 & 0 \\ -c_2 & c_2+c_3 & \cdots & 0 & 0 \\ \vdots & \vdots & \ddots & \vdots & \vdots \\ 0 & 0 & \cdots & -c_n & c_n \end{bmatrix} \tag{1g}$$

$$\mathbf{K}=\begin{bmatrix} k_1+k_2 & -k_2 & \cdots & 0 & 0 \\ -k_2 & k_2+k_3 & \cdots & 0 & 0 \\ \vdots & \vdots & \ddots & \vdots & \vdots \\ 0 & 0 & \cdots & -k_n & k_n \end{bmatrix} \tag{1h}$$

Due to the base isolation, the movement of the main structure (S_r) is very close to one of a rigid body. Thus, it is reasonable to assume that the inter-story motion of the main structure will be much smaller than the absolute motion of the base. Consequently, the following simplified equation of motion of the first floor is obtained

$$m_1\ddot{x}_1(t)+c_1\dot{x}_1(t)+kx_1(t)=c_1\dot{y}(t)+k_1y(t) \tag{1i}$$

In this work, it is assumed that only state variables of the base and the first-floor system are measurable, and the unknown seismic excitation $d(t)$ and $\dot{d}(t)$ are bounded and thus the unknown force $f_{\mathrm{g}}(t)$ in equation (1d) is bounded.

The following propositions about the intrinsic stability of the structure will be used in formulating the control law [**14**].

Proposition 1

The unforced main structure subsystem, i.e. equation (1a) with the null coupling term

$$[c_1, 0, \ldots, 0]^{\mathrm{T}}\dot{y}+[k_1, 0, \ldots, 0]^{\mathrm{T}}y\equiv 0, \qquad t\geqslant 0 \tag{1j}$$

is globally exponentially stable for any bounded initial conditions.

Proposition 2

If the coordinates $(y, \dot{y})$ of the base and the coupling term $[c_1, 0, \ldots, 0]^{\mathrm{T}}\dot{y}+[k_1, 0, \ldots, 0]^{\mathrm{T}}y$ are uniformly bounded, then the main structure subsystem is stable and the coordinates $(x, \dot{x})$ of the main structure are uniformly bounded for all $t \geqslant 0$ and any bounded initial conditions.

2.1 Real-time hybrid testing system

The experimental testing of the control performance in civil engineering structures is an important issue in structural control. It is well known that testing vibration reduction systems at large-scale structures such as buildings or bridges is rather prohibitive because of the dimensions, the power required to do so, and the costs that such tests imply. This is why experiments are usually run at small or mid-scale laboratory specimens. Experiments can be performed in one of three ways: shaking table tests, quasi-static tests, and pseudo-dynamic or hybrid tests [**42**].

One significant advantage of hybrid simulation is that it removes a large source of epistemic uncertainty compared to pure numerical simulations by replacing structural element models that are not well understood with physical specimens on the laboratory test floor [**43**]. There are two main drawbacks with the hybrid test method. First, the method relies on the assumption that the mass of the structure is concentrated at discrete points. Second, the loading is applied over a greatly expanded time scale so that time-dependent nonlinear behaviour is not correctly reproduced in the physical component. In hybrid testing, the displacements are imposed on an extended time scale which typically ranges from 100 to 1000 times the actual earthquake duration to allow for the use of larger actuators without high hydraulic flow requirements, careful observation of the response of the structure during the test, and the ability to pause and resume the experiment. In particular, the method cannot be applied to the testing of highly rate-sensitive components such as visco-elastic dampers and certain active or semi-active structural control devices [**44**].

Figure 2 shows the experimental environment where the system (1) can be tested. Experiments are executed in a real-time hybrid testing (RTHT) configuration available at the Smart Structures Laboratory, University of Illinois at Urbana-Champaign, Illinois, USA. It consists of a computer that both simulates the structure to be controlled and generates the commanding signals (displacements and control signals); a small-scale MR damper that is driven by a hydraulic actuator which in turn is controlled by a servo-hydraulic controller; and DSP, A/D, and D/A hardware for signal processing. Sensors available include a linear variable displacement transformer (LVDT) for displacement measurements and a load cell to measure the MR damper force. In Fig. 2, x_{cmd} is the commanded displacement, f_{mr} is the MR damper force measured by the load cell, x_{meas} is the displacement measured by the LVDT, and i is the control current sent to the hydraulic actuator. A fully detailed description of this RTHT implementation can be found in reference [**45**].

Remark 1

In traditional structural control systems, coaxial wires are normally used to provide communication links between sensors, actuators, and controllers. With the rapid emergence of wireless communication and embedding computing technologies, there has been an increasing interest in the use of wireless

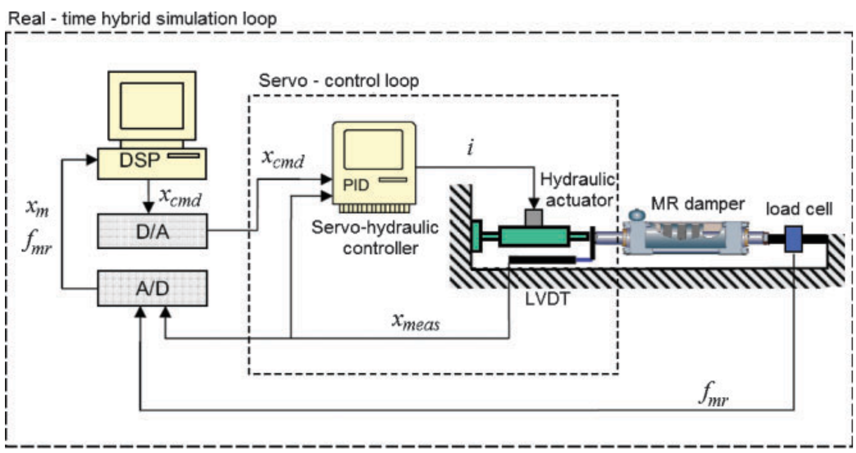

Fig. 2 A schematic of the RTHT system

networks for structural vibration control. The adoption of wireless sensing technologies can remedy the high installation cost of commercial cable-based data acquisition systems. When replacing wired communication channels with wireless ones for feedback structural control, issues such as coordination of sensing and control units, communication range, time delay, and the random packet losses in the sensor-to-controller and controller-to-actuator need to be examined. These issues in the wireless communication usually cause degradation of the real-time performance of a control system. Recently, the robust H_∞ control problem for a class of networked systems with random communication packet losses has been studied in reference [**46**].

3 PROBLEM FORMULATION

In order to design a mixed H_2/H_∞ output-feedback control, the actively controlled base-isolated building system in equation (1) is described by the equations of the form

$$\begin{cases} \hat{\mathbf{M}}\,\ddot{\boldsymbol{X}}_{\text{aug}}(t)+\hat{\mathbf{C}}\,\dot{\boldsymbol{X}}_{\text{aug}}(t)+\hat{\mathbf{K}}\,\boldsymbol{X}_{\text{aug}}(t) \\ \quad =\mathbf{B}_{\text{f}}\,\boldsymbol{f}(t)+\mathbf{B}_{\text{g}}\,\boldsymbol{f}_{\text{g}}(t) & \text{(2a)} \\ \boldsymbol{Z}(t)=\mathbf{C}_1\,\boldsymbol{X}_{\text{aug}}(t)+\mathbf{C}_2\,\dot{\boldsymbol{X}}_{\text{aug}}(t)+\mathbf{D}_1\,\boldsymbol{f}(t) & \text{(2b)} \\ \boldsymbol{Y}(t)=\mathbf{C}_3\,\boldsymbol{X}_{\text{aug}}(t)+\mathbf{C}_4\,\dot{\boldsymbol{X}}_{\text{aug}}(t) & \text{(2c)} \end{cases}$$

with

$$\hat{\mathbf{M}}=\text{diag}\{m_1, m\},\qquad \hat{\mathbf{C}}=\begin{bmatrix} c_1 & -c_1 \\ -c_1 & c_1+c \end{bmatrix}$$

$$\hat{\mathbf{K}}=\begin{bmatrix} k_1 & -k_1 \\ -k_1 & k_1+k \end{bmatrix},\qquad \mathbf{B}_f=\mathbf{B}_g=\begin{bmatrix} 0 \\ 1 \end{bmatrix}$$

where $\boldsymbol{X}_{\text{aug}}(t)=[x_1, y]^{\text{T}}$ is the state vector, $\boldsymbol{f}(t)$ is the control input, $\boldsymbol{f}_{\text{g}}(t)\in L_2[0,\infty)$ is the external disturbance (seismic excitation), $\boldsymbol{Z}(t)\in\Re^s$ is the controlled outputs, and $\boldsymbol{Y}(t)\in\Re^l$ is the measured outputs. The matrices $\mathbf{C}_1$, $\mathbf{C}_2$, $\mathbf{C}_3$, $\mathbf{C}_4$, and $\mathbf{D}_1$ have compatible dimensions and are defined in section 5. In the system (2), taking $\xi(t):=\text{col}(\boldsymbol{X}_{\text{aug}}(t), \dot{\boldsymbol{X}}_{\text{aug}}(t))$ yields an augmented system model, i.e. a first-order linear system

$$\begin{cases} \dot{\xi}(t)=\bar{\mathbf{A}}\,\xi(t)+\bar{\mathbf{B}}_{\text{f}}\,\boldsymbol{f}(t)+\bar{\mathbf{B}}_{\text{g}}\,\boldsymbol{f}_{\text{g}}(t) & \text{(3a)} \\ \boldsymbol{Z}(t)=\tilde{\mathbf{C}}\,\xi(t)+\mathbf{D}_1\,\boldsymbol{f}(t) & \text{(3b)} \\ \boldsymbol{Y}(t)=\bar{\mathbf{C}}\,\xi(t) & \text{(3c)} \end{cases}$$

where

$$\bar{\mathbf{A}}=\begin{bmatrix} 0 & \mathrm{I} \\ -\hat{\mathbf{M}}^{-1}\hat{\mathbf{K}} & -\hat{\mathbf{M}}^{-1}\hat{\mathbf{C}} \end{bmatrix},\qquad \bar{\mathbf{B}}_{\text{f}}=\begin{bmatrix} 0 \\ \hat{\mathbf{M}}^{-1}\mathbf{B}_{\text{f}} \end{bmatrix}$$

$$\bar{\mathbf{B}}_{\text{g}}=\begin{bmatrix} 0 \\ \hat{\mathbf{M}}^{-1}\mathbf{B}_{\text{g}} \end{bmatrix},\qquad \bar{\mathbf{C}}:=[\mathbf{C}_3, \mathbf{C}_4],\qquad \tilde{\mathbf{C}}:=[\mathbf{C}_1, \mathbf{C}_2]$$

Definition 1

1. The H_2 performance measure of the system (3) is defined as

$$J_2=\int_0^\infty\left[\xi^{\text{T}}(t)\mathbf{S}_1\,\xi(t)+\boldsymbol{f}^{\text{T}}(t)\mathbf{S}_2\,\boldsymbol{f}(t)\right]\text{d}t$$

   where $\boldsymbol{f}_{\text{g}}(t)\equiv 0$ and constant matrices $\mathbf{S}_1$, $\mathbf{S}_2>0$ are given.
2. The H_∞ performance (or L_2-gain) measure of the system (3) is defined as

$$J_\infty=\int_0^\infty\left[\boldsymbol{Z}^{\text{T}}(t)\,\boldsymbol{Z}(t)-\gamma^2\boldsymbol{f}_{\text{g}}^{\text{T}}(t)\,\boldsymbol{f}_{\text{g}}(t)\right]\text{d}t$$

   where the positive scalar γ is given.
3. The mixed H_2/H_∞ performance measure of the system (3) is defined as

$$\min(J_0|\,J_\infty<0 \text{ and } J_2\leqslant J_0)$$

   or the so-called problem of minimizing an upper bound of J_2, i.e. $J_0>0$, under the constraint $J_\infty<0$.

Remark 2

The minimization of J_2 will result in the reduction of the structural response and control effort while the accomplishment of $J_\infty<0$ will maintain the structural response within the quadratic-type performance under a prescribed γ-level L_2-gain in the presence of external disturbances. Although the robust H_∞ design is mainly related to robust stability and frequency domain performance specifications, it does not seriously address the transient behaviour which is also important in the control. Therefore, based on mixed H_2/H_∞ optimization, a controller is designed which explicitly trades between nominal performance and robust stability. To date, several approaches have been proposed to solve the mixed H_2/H_∞ control problem; a Nash game-theoretic approach was proposed to solve the mixed H_2/H_∞ control problem of deterministic linear systems through a set of cross-coupled Riccati equations [47]. This method has been generalized to non-linear [48], output feedback control [49], and stochastic systems [50–52]. The problem of controller design to be addressed in this paper is formulated as follows: given the second-order linear system (3) with a prescribed level of disturbance attenuation $\gamma > 0$, find a mixed H_2/H_∞ output-feedback control $\boldsymbol{f}(t)$ of the form

$$\boldsymbol{f}(t) = \mathbf{K}_{\mathrm{f}} \boldsymbol{Y}(t) \tag{4}$$

where the matrix $\mathbf{K}_{\mathrm{f}}$ is the control gain to be determined such that the following conditions are met.

1. The resulting closed-loop system (3) and (4) is asymptotically stable.
2. Under $\boldsymbol{f}_{\mathrm{g}}(t) \equiv 0$, the H_2 performance measure satisfies $J_2 \leqslant J_0$, where the positive scalar J_0 is said to be a guaranteed cost.
3. Under zero initial conditions and for all non-zero $\boldsymbol{f}_{\mathrm{g}}(t) \in L_2[0, \infty)$, the upper bound of the H_2 performance measure, i.e. J_0, satisfies $J_\infty < 0$ (or the induced L_2-norm of the operator from $\boldsymbol{f}_{\mathrm{g}}(t)$ to the controlled outputs $\boldsymbol{Z}(t)$ is less than γ).

In this case, the second-order linear system (3) is said to be asymptotically stable with a mixed H_2/H_∞ performance measure.

Remark 3

Note that the H_∞ norm of the transfer function $\mathbf{H}(s) = (\tilde{\mathbf{C}} + \mathbf{D}_1\mathbf{K}_{\mathrm{f}}\bar{\mathbf{C}})(s\mathbf{I} - \bar{\mathbf{A}} - \bar{\mathbf{B}}_{\mathrm{f}}\mathbf{K}_{\mathrm{f}}\bar{\mathbf{C}})^{-1}\bar{\mathbf{B}}_{\mathrm{g}}$ from the disturbance input $\boldsymbol{f}_{\mathrm{g}}(t)$ to the controlled outputs $\boldsymbol{Z}(t)$ satisfies the constraint

$$\|\boldsymbol{H}(s)\|_\infty = \sup_{\boldsymbol{f}_{\mathrm{g}} \in L_2} \|\boldsymbol{Z}(t)\|_2 \Big/ \left\|\boldsymbol{f}_{\mathrm{g}}(t)\right\|_2 \leqslant \gamma$$

where $\|\boldsymbol{H}(s)\|_\infty = \sup_{\omega \in \Re} \sigma_{\max}[H(j\omega)]$. Therefore, minimizing the H_∞ norm corresponds to minimizing the peak of the largest singular value.

Remark 4

In practice, it may be more desirable to directly influence the minimization of the maximum absolute values of control inputs, the response overshoot, or other time domain properties of the system response (namely the L_∞-gain) rather than the energy where the disturbance input is also of finite L_∞-norm. In this case, the aim is to satisfy the following induced-L_∞ norm condition

$$\|\boldsymbol{H}(s)\|_{\infty-\mathrm{ind}} := \sup_{\boldsymbol{f}_{\mathrm{g}} \in L_2} \frac{\|\boldsymbol{Z}(t)\|_\infty}{\left\|\boldsymbol{f}_{\mathrm{g}}(t)\right\|_\infty} \leqslant \gamma$$

In such cases an induced-L_∞ norm is obtained which is often referred to as an L_1 problem due to the fact that the induced-L_∞ norm for a linear system is just the L_1-norm of its impulse response and an upper bound on the L_1-norm of the transfer function. Therefore, the name L_1-optimal control is used for the filed of L_∞-gain-based disturbance attenuation [53].

4 MAIN RESULTS

In this section, sufficient conditions for the solvability of the H_∞ control design problem are proposed using the Lyapunov method and an LMI approach.

First, equation (3a) is represented in an equivalent descriptor model form as

$$\begin{cases} \dot{\xi}(t) = \boldsymbol{\eta}(t) \\ 0 = -\boldsymbol{\eta}(t) + \left(\bar{\mathbf{A}} + \bar{\mathbf{B}}_{\mathrm{f}}\mathbf{K}_{\mathrm{f}}\bar{\mathbf{C}}\right)\xi(t) + \bar{\mathbf{B}}_{\mathrm{g}}\boldsymbol{f}_{\mathrm{g}}(t) \end{cases} \tag{5}$$

Define the Lyapunov–Krasovskii functional

$$V(t) = \xi(t)^{\mathrm{T}}\mathbf{P}_1\xi(t) := \begin{bmatrix} \xi(t)^{\mathrm{T}} & \boldsymbol{\eta}(t)^{\mathrm{T}} \end{bmatrix} \mathbf{T}\,\mathbf{P} \begin{bmatrix} \xi(t) \\ \boldsymbol{\eta}(t) \end{bmatrix} \tag{6}$$

with $\mathbf{T} = \operatorname{diag}\{\mathbf{I}, 0\}$ and

$$\mathbf{P} = \begin{bmatrix} \mathbf{P}_1 & 0 \\ \mathbf{P}_3 & \mathbf{P}_2 \end{bmatrix}$$

when $\mathbf{P}_1 = \mathbf{P}_1^{\mathrm{T}} > 0$. Differentiating $V(t)$ along the system trajectory becomes

$$\begin{aligned} \dot{V}(t) &= 2\xi(t)^{\mathrm{T}}\mathbf{P}_1\dot{\xi}(t) = 2\begin{bmatrix} \xi(t)^{\mathrm{T}} & \boldsymbol{\eta}(t)^{\mathrm{T}} \end{bmatrix}\mathbf{P}^{\mathrm{T}}\begin{bmatrix} \dot{\xi}(t) \\ 0 \end{bmatrix} \\ &= 2\begin{bmatrix} \xi(t)^{\mathrm{T}} & \boldsymbol{\eta}(t)^{\mathrm{T}} \end{bmatrix} \\ &\quad \times \mathbf{P}^{\mathrm{T}}\begin{bmatrix} \boldsymbol{\eta}(t) \\ -\boldsymbol{\eta}(t) + \left(\bar{\mathbf{A}} + \bar{\mathbf{B}}_{\mathrm{f}}\mathbf{K}_{\mathrm{f}}\bar{\mathbf{C}}\right)\xi(t) + \bar{\mathbf{B}}_{\mathrm{g}}\boldsymbol{f}_{g}(t) \end{bmatrix} \\ &= 2\begin{bmatrix} \xi(t)^{\mathrm{T}} & \boldsymbol{\eta}(t)^{\mathrm{T}} \end{bmatrix} \\ &\quad \times \mathbf{P}^{\mathrm{T}}\left(\begin{bmatrix} 0 & \mathbf{I} \\ \bar{\mathbf{A}} + \bar{\mathbf{B}}_{\mathrm{f}}\mathbf{K}_{\mathrm{f}}\bar{\mathbf{C}} & -\mathbf{I} \end{bmatrix}\begin{bmatrix} \xi(t) \\ \boldsymbol{\eta}(t) \end{bmatrix} + \begin{bmatrix} 0 \\ \bar{\mathbf{B}}_{\mathrm{g}} \end{bmatrix}\boldsymbol{f}_{\mathrm{g}}(t)\right) \end{aligned} \tag{7}$$

On the other hand, under zero initial conditions the H_∞ performance measure can be rewritten as

$$J_{\infty} \leqslant \int_0^{\infty} \left[\boldsymbol{Z}(t)^{\mathrm{T}} \boldsymbol{Z}(t) - \gamma^2 \boldsymbol{f}_{\mathrm{g}}(t)^{\mathrm{T}} \boldsymbol{f}_{\mathrm{g}}(t) \right] \mathrm{d}t - V(t)|_{t=0} + V(t)|_{t=\infty} = \int_0^{\infty} \left[\boldsymbol{Z}(t)^{\mathrm{T}} \boldsymbol{Z}(t) - \gamma^2 \boldsymbol{f}_{\mathrm{g}}(t)^{\mathrm{T}} \boldsymbol{f}_{\mathrm{g}}(t) + \dot{V}(t) \right] \mathrm{d}t \tag{8}$$

Substituting the term of

$$\boldsymbol{Z}(t) = \tilde{\mathbf{C}}\xi(t) + \mathbf{D}_1 \boldsymbol{f}(t) = \left(\tilde{\mathbf{C}} + \mathbf{D}_1 \mathbf{K}_{\mathrm{f}} \bar{\mathbf{C}}\right)\xi(t) \tag{9}$$

in equation (8) results in the inequality

$$J_{\infty} \leqslant \int_0^{\infty} \vartheta(s)^{\mathrm{T}} \mathbf{\Pi}_1 \vartheta(s)\ \mathrm{d}s$$

where

$$\vartheta(t) := \mathrm{col}\left\{ \xi_{\mathrm{c}}(t), \boldsymbol{\eta}(t), \boldsymbol{f}_{\mathrm{g}}(t) \right\}$$

and the matrix $\mathbf{\Pi}_1$ is given by

$$\mathbf{\Pi}_1 := \begin{bmatrix} \mathrm{sym}\left(\mathbf{P}^{\mathrm{T}} \begin{bmatrix} 0 & \mathbf{I} \\ \bar{\mathbf{A}} + \bar{\mathbf{B}}_{\mathrm{f}} \mathbf{K}_{\mathrm{f}} \bar{\mathbf{C}} & -\mathbf{I} \end{bmatrix} \right) + \begin{bmatrix} \left(\tilde{\mathbf{C}} + \mathbf{D}_1 \mathbf{K}_{\mathrm{f}} \bar{\mathbf{C}}\right)^{\mathrm{T}} \left(\tilde{\mathbf{C}} + \mathbf{D}_1 \mathbf{K}_{\mathrm{f}} \bar{\mathbf{C}}\right) & 0 \\ 0 & 0 \end{bmatrix} & \mathbf{P}^{\mathrm{T}} \begin{bmatrix} 0 \\ \bar{\mathbf{B}}_{\mathrm{g}} \end{bmatrix} \\ * & -\gamma^2 \mathbf{I} \end{bmatrix} \tag{10}$$

Now, if $\mathbf{\Pi}_1 < 0$ then $J_{\infty} < 0$, which means that the L_2-gain from the disturbance $\boldsymbol{f}_{\mathrm{g}}(t)$ to the controlled output $\boldsymbol{Z}(t)$ is less than γ. By applying the Schur complement on the first element of the matrix $\mathbf{\Pi}_1$, one obtains $\mathbf{\Pi}_1 < 0$ which is equivalent to

$$\begin{bmatrix} \mathrm{sym}\left(\mathbf{P}^{\mathrm{T}} \begin{bmatrix} 0 & \mathbf{I} \\ \bar{\mathbf{A}} + \bar{\mathbf{B}}_{\mathrm{f}} \mathbf{K}_{\mathrm{f}} \bar{\mathbf{C}} & -\mathbf{I} \end{bmatrix} \right) & \mathbf{P}^{\mathrm{T}} \begin{bmatrix} 0 \\ \bar{\mathbf{B}}_{\mathrm{g}} \end{bmatrix} & \begin{bmatrix} \left(\tilde{\mathbf{C}} + \mathbf{D}_1 \mathbf{K}_{\mathrm{f}} \bar{\mathbf{C}}\right)^{\mathrm{T}} \\ 0 \end{bmatrix} \\ * & -\gamma^2 \mathbf{I} & 0 \\ * & * & -\mathbf{I} \end{bmatrix} < 0 \tag{11}$$

It is also easy to see that the inequality above implies $\mathrm{sym}\left(\mathbf{P}_2^{\mathrm{T}}\right) < 0$. Hence, the matrices $\mathbf{P}$ and $\mathbf{P}_2$ are non-singular. Then, according to the structure of the matrix $\mathbf{P}$, the matrix $\mathbf{X} := \mathbf{P}^{-1}$ has the form

$$\mathbf{X} = \begin{bmatrix} \mathbf{X}_1 & 0 \\ \mathbf{X}_3 & \mathbf{X}_2 \end{bmatrix} \tag{12}$$

where $\mathbf{X}_i = \mathbf{P}_i^{-1} (i = 1, 2)$ and $\mathbf{X}_3 = -\mathbf{X}_2 \mathbf{P}_3 \mathbf{X}_1$. Let $\zeta = \mathrm{diag}\{\mathbf{X}^{\mathrm{T}}, \mathbf{I}, \mathbf{X}_1\}$. Premultiplying ζ and postmultiplying ζ^{T} to the inequality (11) and considering $\bar{\mathbf{C}}\mathbf{X}_1 = \hat{\mathbf{X}}_1 \bar{\mathbf{C}}$ according to Lemma 1 (in the Appendix), obtains

$$\begin{bmatrix} \mathrm{sym}\left(\begin{bmatrix} \mathbf{X}_3 & \mathbf{X}_2 \\ \bar{\mathbf{A}}\mathbf{X}_1 + \bar{\mathbf{B}}_{\mathrm{f}} \mathbf{K}_{\mathrm{f}} \hat{\mathbf{X}}_1 \bar{\mathbf{C}} - \mathbf{X}_3 & -\mathbf{X}_2 \end{bmatrix} \right) & \begin{bmatrix} 0 \\ \bar{\mathbf{B}}_{\mathrm{g}} \end{bmatrix} & \begin{bmatrix} \left(\tilde{\mathbf{C}}\mathbf{X}_1 + \mathbf{D}_1 \mathbf{K}_{\mathrm{f}} \hat{\mathbf{X}}_1 \bar{\mathbf{C}}\right)^{\mathrm{T}} \\ 0 \end{bmatrix} \\ * & -\gamma^2 \mathbf{I} & 0 \\ * & * & -\mathbf{I} \end{bmatrix} < 0 \tag{13}$$

Obviously, the matrix inequality (13) includes multiplication of control gain and the decision variable $\hat{\mathbf{X}}_1$. Now, by considering $\mathbf{K}_f\hat{\mathbf{X}}_1 = \tilde{\mathbf{X}}_1$ the matrix inequality (13) is converted into a convex programming problem written in terms of LMI as follows

$$\begin{bmatrix} \mathrm{sym}\left(\begin{bmatrix} \mathbf{X}_3 & \mathbf{X}_2 \\ \bar{\mathbf{A}}\mathbf{X}_1 + \bar{\mathbf{B}}_f\tilde{\mathbf{X}}_1\bar{\mathbf{C}} - \mathbf{X}_3 & -\mathbf{X}_2 \end{bmatrix}\right) & \begin{bmatrix} 0 \\ \bar{\mathbf{B}}_g \end{bmatrix} & \begin{bmatrix} \left(\tilde{\mathbf{C}}\mathbf{X}_1 + \mathbf{D}_1\tilde{\mathbf{X}}_1\bar{\mathbf{C}}\right)^{\mathrm{T}} \\ 0 \end{bmatrix} \\ * & -\gamma^2\mathbf{I} & 0 \\ * & * & -\mathbf{I} \end{bmatrix} < 0 \tag{14}$$

On the other hand, by applying the same Lyapunov function (6) for the second-order linear system (3), under $\boldsymbol{f}_g(t) \equiv 0$, for the index J_2 in definition 1 gives

$$J_2 \leqslant \int_0^\infty \left[\xi^{\mathrm{T}}(t)\mathbf{S}_1\xi(t) + \xi^{\mathrm{T}}(t)\mathbf{C}^{\mathrm{T}}\mathbf{K}_f^{\mathrm{T}}\mathbf{S}_2\mathbf{K}_f\mathbf{C}\xi(t) + \dot{V}(t)\right] \mathrm{d}t$$

$$\leqslant \int_0^\infty \hat{\boldsymbol{\vartheta}}^{\mathrm{T}}(t)\boldsymbol{\Pi}_2\hat{\boldsymbol{\vartheta}}(t)\, \mathrm{d}t \tag{15}$$

where $\hat{\boldsymbol{\vartheta}}(t) := \mathrm{col}\{\xi(t), \boldsymbol{\eta}(t)\}$ and the matrix $\boldsymbol{\Pi}_2$ is given by

$$\boldsymbol{\Pi}_2 := \mathrm{sym}\left(\mathbf{P}^{\mathrm{T}}\begin{bmatrix} 0 & \mathbf{I} \\ \bar{\mathbf{A}} + \bar{\mathbf{B}}_f\mathbf{K}_f\bar{\mathbf{C}} & -\mathbf{I} \end{bmatrix}\right) + \begin{bmatrix} \mathbf{S}_1 + \left(\mathbf{K}_f\bar{\mathbf{C}}\right)^{\mathrm{T}}\mathbf{S}_2\left(\mathbf{K}_f\bar{\mathbf{C}}\right) & 0 \\ 0 & 0 \end{bmatrix}$$

$$\int_0^\infty \dot{V}(t)\, \mathrm{d}t = \lim_{t\to\infty} V(t) - V(0)$$

$$\leqslant -\int_0^\infty \left[\xi^{\mathrm{T}}(t)\mathbf{S}_1\xi(t) + \xi^{\mathrm{T}}(t)\mathbf{C}^{\mathrm{T}}\mathbf{K}_f^{\mathrm{T}}\mathbf{S}_2\mathbf{K}_f\mathbf{C}\xi(t)\right] \mathrm{d}t \tag{17}$$

Now, the H_2 performance measure for the system (3) is established as

$$\int_0^\infty \left[\xi^{\mathrm{T}}(t)\mathbf{S}_1\xi(t) + \xi^{\mathrm{T}}(t)\mathbf{C}^{\mathrm{T}}\mathbf{K}_f^{\mathrm{T}}\mathbf{S}_2\mathbf{K}_f\mathbf{C}\xi(t)\right] \mathrm{d}t$$

$$\leqslant V(0) = J_0 \tag{18}$$

where $J_0 = \xi(0)^{\mathrm{T}}\mathbf{P}_1\xi(0)$. Similarly, using the Schur complement the inequality $\boldsymbol{\Pi}_2 < 0$ yields

$$\begin{bmatrix} \mathrm{sym}\left(\mathbf{P}^{\mathrm{T}}\begin{bmatrix} 0 & \mathbf{I} \\ \bar{\mathbf{A}} + \bar{\mathbf{B}}_f\mathbf{K}_f\bar{\mathbf{C}} & -\mathbf{I} \end{bmatrix}\right) + \begin{bmatrix} \mathbf{S}_1 & 0 \\ 0 & 0 \end{bmatrix} & \begin{bmatrix} \left(\mathbf{K}_f\bar{\mathbf{C}}\right)^{\mathrm{T}} \\ 0 \end{bmatrix}\mathbf{S}_2 \\ * & -\mathbf{S}_2 \end{bmatrix} < 0 \tag{19}$$

Again, by applying the congruence transformation $\mathrm{diag}\{\mathbf{X}^{\mathrm{T}}, \mathbf{I}\}$ to the matrix inequality above, readily obtains the following LMI

$$\begin{bmatrix} \mathrm{sym}\left(\begin{bmatrix} \mathbf{X}_3 & \mathbf{X}_2 \\ \bar{\mathbf{A}}\mathbf{X}_1 + \bar{\mathbf{B}}_f\tilde{\mathbf{X}}_1\bar{\mathbf{C}} - \mathbf{X}_3 & -\mathbf{X}_2 \end{bmatrix}\right) & \begin{bmatrix} \left(\tilde{\mathbf{X}}_1\bar{\mathbf{C}}\right)^{\mathrm{T}} \\ 0 \end{bmatrix}\mathbf{S}_2 & \begin{bmatrix} \mathbf{X}_1\mathbf{S}_1 \\ 0 \end{bmatrix} \\ * & -\mathbf{S}_2 & 0 \\ * & * & -\mathbf{S}_1 \end{bmatrix} < 0 \tag{20}$$

Therefore, the condition $\boldsymbol{\Pi}_2 < 0$ in equation (15) implies

$$\dot{V}(t) \leqslant -\xi^{\mathrm{T}}(t)\mathbf{S}_1\xi(t) - \xi^{\mathrm{T}}(t)\mathbf{C}^{\mathrm{T}}\mathbf{K}_f^{\mathrm{T}}\mathbf{S}_2\mathbf{K}_f\mathbf{C}\xi(t) \tag{16}$$

or equivalently

Finally, the results are summarized as follows.

Theorem 1

Consider the base-isolated building structure (3) with $\mathrm{rank}(\bar{\mathbf{C}}) = p < 2(n+1)$. For given a scalar γ, there exists a mixed H_2/H_∞ output-feedback control in the form of equation (4) such that the resulting closed-loop system is robustly asymptotically stable and satisfies the constraint $J_2 \leqslant J_0$ under the constraint $J_\infty < 0$, if there exist matrices $\mathbf{X}_2$, $\mathbf{X}_3$, $\tilde{\mathbf{X}}_1$ and positive-definite matrices $\mathbf{X}_{11}, \mathbf{X}_{22}$ satisfying the LMIs (14) and (20). The desired control gain in equation (4) is given by

$$\mathbf{K}_\mathrm{f} = \tilde{\mathbf{X}}_1 \hat{\mathbf{X}}_1^{-1} \quad \text{from LMIs (14) and (20)} \tag{21}$$

where $\bar{\mathbf{C}} = \mathrm{U}[\hat{\mathbf{C}} \quad 0]\mathbf{V}^\mathrm{T}$ and

$$\mathbf{X}_1 = \mathbf{V}\begin{bmatrix} \mathbf{X}_{11} & 0 \\ 0 & \mathbf{X}_{22} \end{bmatrix}\mathbf{V}^\mathrm{T}$$

and $\hat{\mathbf{X}}_1 = \mathbf{U}\hat{\mathbf{C}}\mathbf{X}_{11}\hat{\mathbf{C}}^{-1}\mathbf{U}^\mathrm{T}$ with $\mathbf{X}_{11} \in \Re^{p\times p}$, $\mathbf{X}_{22} \in \Re^{(2n-p+2)\times(2n-p+2)}$, the unitary matrices $\mathbf{U} \in \Re^{p\times p}$, $\mathbf{V} \in \Re^{2(n+1)\times 2(n+1)}$, and a diagonal matrix $\hat{\mathbf{C}} \in \Re^{p\times p}$ with positive diagonal elements in decreasing order. Moreover, an upper bound of the H_2 performance measure is obtained by $J_0 = \xi(0)^\mathrm{T}\mathbf{X}_1^{-1}\xi(0)$.

Remark 5

If $\mathrm{rank}(\bar{\mathbf{C}}) = l = 2(n+1)$, the matrix $\bar{\mathbf{C}}$ is non-singular, it is clear that the matrix equation $\bar{\mathbf{C}}\mathbf{X}_1 = \hat{\mathbf{X}}_1\bar{\mathbf{C}}$ is solvable on $\hat{\mathbf{X}}_1$, i.e. $\hat{\mathbf{X}}_1 = \bar{\mathbf{C}}\mathbf{X}_1\bar{\mathbf{C}}^{-1}$. In this case, the results of Theorem 1 are true for a full (non-diagonal) matrix $\mathbf{X}_1$, that is

$$\mathbf{X}_1 = \begin{bmatrix} \mathbf{X}_{11} & \mathbf{X}_{12} \\ * & \mathbf{X}_{22} \end{bmatrix}$$

and the desired control gain in equation (21) is given by $\mathbf{K}_\mathrm{f} = \tilde{\mathbf{X}}_1\bar{\mathbf{C}}\mathbf{X}_1^{-1}\bar{\mathbf{C}}^{-1}$.

Remark 6

Minimizing the upper bound of the H_2 performance measure is stated in the following convex optimization problem

min α

subject to

(i) LMIs (14) and (20)
(ii) $\begin{bmatrix} -\alpha & \xi(0)^\mathrm{T} \\ * & -\mathbf{X}_1 \end{bmatrix} < 0$

5 SIMULATION RESULTS

The controller was implemented using the following numerical values. the mass and stiffness of the base are $m = 6\times 10^5$ kg, $k = 1.184\times 10^7$ N/m, and the base damping coefficient is 0.1, respectively; the main structure stiffness varies linearly from the first floor $k_1 = 9\times 10^8$ N/m to the top floor $k_{10} = 4.5\times 10^8$ N/m; the damping coefficient is 0.05 and the passive actuator has the following values: $Q = \sum_{i=1}^{10} m_i$, $\mu_{\max} = 0.185$, $\Delta\mu = 0.09$, and $v = 2.0$.

To design a robust mixed H_2/H_∞ control law (4), we solved LMIs (14) and (20) using MATLAB LMI Control Toolbox [**54**] in the case of $\boldsymbol{Z}(t) = [\xi(t)^\mathrm{T}, \boldsymbol{f}(t)^\mathrm{T}]^\mathrm{T}$, $\mathbf{C}_3 = [\mathbf{I}_2,\ 0_{2\times 2}]^\mathrm{T}$, $\mathbf{C}_4 = [0_{2\times 2},\ \mathbf{I}_2]^\mathrm{T}$, $\mathbf{S}_1 = \mathbf{I}$, and $\mathbf{S}_2 = \mathbf{I}$, and obtained the minimum value of the parameter γ in optimal H_∞ performance measure as 1.05.

For the initial condition $\xi(0) = (0, 0, 0.2, 0, 0.1, 0, 0.1, 0)^\mathrm{T}$ and considering the Taft earthquake records (see Fig. 3) as a disturbance, Figs 4 and 5 show the results of both 'passive base isolation' and 'passive base isolation plus active control' compared to that of the system without control; and the corresponding suboptimal H_2 performance measure of the closed-loop system is $J_0 = 7.3430$. In both cases, a reduction in absolute displacement and velocity is achieved with better results when the active control device is integrated. Finally, Fig. 6

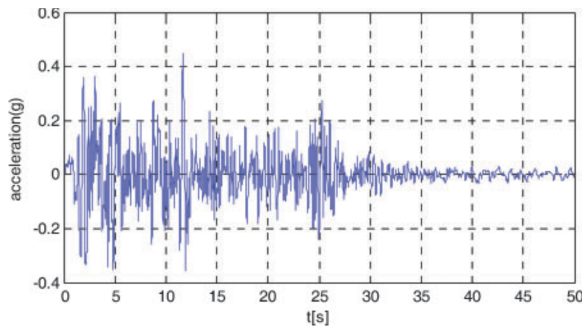

Fig. 3 The Taft earthquake records

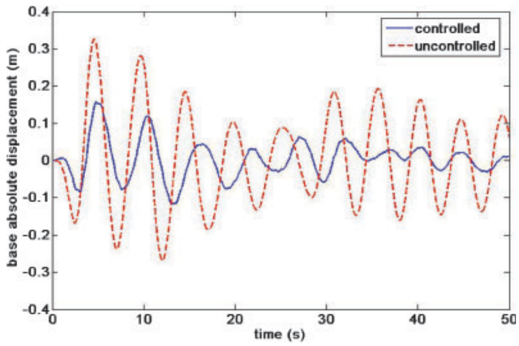

Fig. 4 Horizontal absolute base displacement

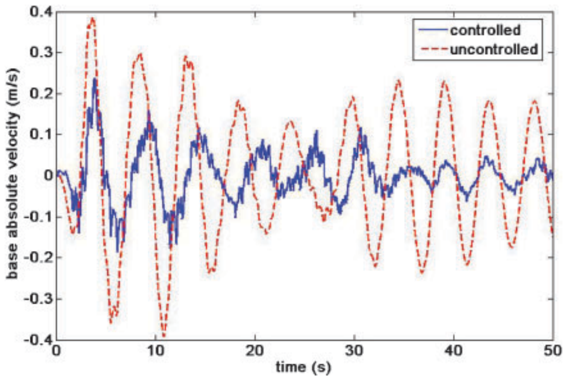

Fig. 5 Horizontal absolute base velocity

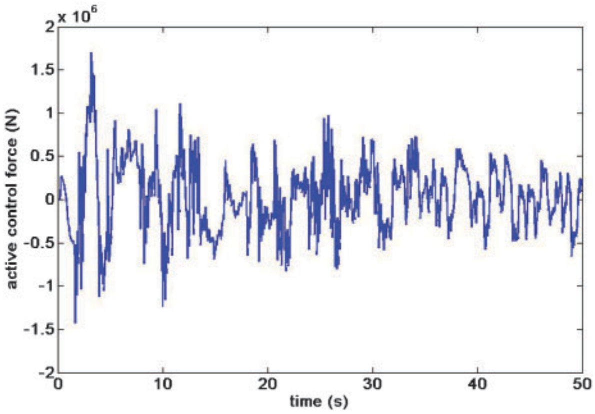

Fig. 6 Active control force

shows the active control effort which is within the limits of practical devices.

6 CONCLUSIONS AND FUTURE WORK

In this paper a mixed H_2/H_∞ output-feedback controller for vibration reduction of uncertain structures modelled in the form of second-order linear systems was developed. Sufficient conditions for the design of a desired control were given in terms of LMIs. A controller which guarantees asymptotic stability and a mixed H_2/H_∞ performance for the closed-loop system of the structure was developed based on a Lyapunov function. The performance of the controller was evaluated by means of simulations in MATLAB/Simulink. Future work will investigate the mixed H_2/H_∞ control design for vibration structures by considering the dynamics of actuators which insert some non-linear terms into the model.

ACKNOWLEDGEMENTS

This work has been partially funded by the European Union (European Regional Development Fund) and the Ministry of Science and Innovation (Spain) through the coordinated research project DPI2008-06699-C02. The author Mauricio Zapateiro is grateful for a FI grant from the Department for Innovation, University and Enterprise of the Government of Catalonia, Spain. The authors would like to thank the anonymous reviewers for their constructive comments and suggestions, which improved the quality of the paper.

REFERENCES

1 **Yoshioka, H., Ramallo, J.,** and **Spencer, B.** Smart based isolation strategies employing magnetorheological dampers. *J. Engng Mech.*, 2002, **128**, 540–551.
2 **Spencer, B.** and **Sain, M.** Controlling buildings: a new frontier in feedback. *IEEE Control Syst. Mag.*, 1997, **17**, 19–35.
3 **Dyke Jr, S., Spencer, B., Sain, M.,** and **Carlson, J.** An experimental study of MR dampers for seismic protection. *Smart Mater. Struct.*, 1998, **7**, 693–703.
4 **Spencer, B.** and **Song, T.** New applications and development of active, semi-active and hybrid control techniques for seismic and non-seismic vibration in the USA. In Proceedings of the International Post-SMIRT Conference Seminar on *Seismic isolation, passive energy dissipation and active control of vibration of structures*, Cheju, Korea, 1999.
5 **Du, H., Kam Sze, Y.,** and **Lam, J.** Semi-active H_∞ control of vehicle suspension with magneto-rheological dampers. *J. Sound Vib.*, 2005, **283**, 981–996.
6 **Karimi, H. R., Zapateiro, M.,** and **Luo, N.** Wavelet-based parameter identification of a nonlinear magnetorheological damper. *Int. J. Wave., Multires. Image Process.*, 2009, **7**(2), 183–198.
7 **Alvin, K. F.** and **Park, K. C.** Second-order structural identification procedure via state-space-based system identification. *AIAA J.*, 1994, **32**(2), 397–406.
8 **Friswell, M. I.** Extracting second-order systems from state-space representations. *AIAA J.*, 1999, **37**(1), 132–135.
9 **Garrard, W. L.** and **Walker, J. A.** Stability of a class of coupled systems. *IEEE Trans. Autom. Control*, 1967, **12**(6), 786–787.
10 **Henrion, D., Sebek, M.,** and **Kucera, V.** Robust pole placement for second-order systems: an LMI approach. October 2002, available from http://citeseer.ist.psu.edu/623785.html.
11 **Datta, B. N.** and **Rincon, F.** Feedback stabilization of a second-order system: a nonmodal approach. *Linear Algebr. Appl.*, 1993, **188**, 138–161.
12 **Duan, G. R.** Parametric eigenstructure assignment in second-order descriptor linear systems. *IEEE Trans. Autom. Control*, 2004, **49**(10), 1789–1795.

13 **Karimi, H. R.** Optimal vibration control of vehicle engine-body system using Haar functions. *Int. J. Control, Autom. Syst.*, 2006, **4**(6), 714–724.
14 **Luo, N., Rodellar, J., de la Sen, M.,** and **Vehi, J.** Output feedback sliding mode control of base isolated structures. *J. Franklin Inst.*, 2000, **337**, 555–577.
15 **Yang, J. N., Lin, S.,** and **Jabbari, F.** H_2 based control strategies for civil engineering structures. *J. Struct. Control*, 2003, **10**, 205–230.
16 **Yang, J. N., Lin, S.,** and **Jabbari, F.** H_∞ based control strategies for civil engineering structures. *Struct. Control Health Monit.*, 2004, **11**, 223–237.
17 **Karimi, H. R., Zapateiro, M.,** and **Luo, N.** A linear matrix inequality approach to H_∞ control of vehicle engine-body vibration systems with a time-varying actuator delay. *Proc. IMechE, Part I: J. Systems and Control Engineering*, 2008, **222**(I8), 883–899. DOI: 10.1243/09596518JSCE620.
18 **Karimi, H. R.** and **Gao, H.** LMI-based delay-dependent mixed H_2/H_∞ control of second-order neutral systems with time-varying state and input delays. *ISA Trans.*, 2008, **47**(3), 311–324.
19 **Chen, Y.** and **Zhu, C.** Active vibration control based on linear matrix inequality for rotor system under seismic excitation. *J. Sound Vib.*, 2008, **314**, 53–69.
20 **Hong, S., Park, C. H.,** and **Park, H. C.** Vibration control of beams using multiobjective state-feedback control. *Smart Mater. Struct.*, 2006, **15**, 157–163.
21 **Gao, H., Lam, J.,** and **Wang, C.** Multi-objective control of vehicle active suspension systems via load-dependent controllers. *J. Sound Vibr.*, 2006, **290**, 654–675.
22 **Wang, Z., Zeng, H., Ho, D. W. C.,** and **Unbehauen, H.** Multiobjective control of a four-link flexible manipulator: a robust H_∞ approach. *IEEE Trans. Control Syst. Technol.*, 2002, **10**(6), 866–875.
23 **Wang, Z.** Robust H_∞ state feedback control with regional pole constraints: an algebraic Riccati equation approach. *Trans. ASME: J. Dyn. Syst., Meas. Control*, 1998, **120**(2), 289–292.
24 **Wang, Z., Tang, G.,** and **Chen, X.** Robust controller design for uncertain linear systems with circular pole constraints. *Int. J. Control*, 1996, **65**(6), 1045–1054.
25 **Zapateiro, M., Luo, N.,** and **Karimi, H. R.** Semi-active control of a base isolated building using magnetorheological dampers. *Int. J. Model., Identif. Control*, 2009, **7**(1), 41–48.
26 **Dyke, S., Spencer, B., Sain, M.,** and **Carlson, J.** Modeling and control of magnetorheological dampers for seismic response reduction. *Smart Mater. Struct.*, 1996, **5**, 565–575.
27 **Jansen, L.** and **Dyke, S.** Semiactive control strategies for MR dampers: comparative study. *J. Engng Mech.*, 2000, **126**, 795–803.
28 **Yang, G.** *Large-scale magnetorheological fluid damper for vibration mitigation: modeling, testing and control*. PhD Thesis, University of Notre Dame, 2001.
29 **Wang, X.** and **Gordaninejad, F.** Lyapunov-based control of a bridge using magnetorheological fluid dampers. *J. Intell. Mater. Syst. Struct.*, 2002, **13**, 415–419.
30 **Park, C.** and **Jeon, D.** Semiactive vibration control of a smart seat with an MR fluid damper considering its time delay. *J. Intell. Mater. Syst. Struct.*, 2002, **13**, 521–524.
31 **Luo, N., Villamizar, R., Vehi, J., Rodellar, J.,** and **Manosa, V.** Sliding mode control of structures with uncertain coupled subsystems and actuator dynamics. In Proceedings of the *European control conference*, Cambridge, UK, 1–4 September 2003.
32 **Nagarajaiah, S., Narasimhan, S., Agrawal, A.,** and **Tang, P.** Semiactive Lyapunov controller for phase II seismic isolated bridge benchmark. Structures Congress 2006, St. Louis, Missouri, USA, 2006.
33 **McClamroch, N., Gavin, H., Ortiz, D.,** and **Hanson, R.** Electrorheological dampers and semi-active structural control. In Proceedings of the 33rd Conference on *Decision and control*, Florida, USA, 14–16 December 1994, vol. 1, pp. 97–102.
34 **McClamroch, N.** and **Gavin, H.** Closed loop structural control using electrorheological dampers. In Proceedings of the *American control conference*, Seattle, Washington, June 1995, pp. 4173–4177.
35 **Villamizar, R., Luo, N., Vehi, J.,** and **Rodellar, J.** Semiactive sliding mode control of uncertain base isolated structures with actuator dynamics. In Proceedings of the AMAS/ECCOMAS/STC Workshop on Smart Materials and Structures (ECCOMAS-SMART), Jadwisin, Poland, 2–5 September 2003, pp. 224–231.
36 **Moon, S., Bergman, L.,** and **Voulgaris, P.** Sliding mode control of cable-stayed bridge subjected to seismic excitation. *J. Engng Mech.*, 2003, **129**, 71–78.
37 **Luo, N., Villamizar, R.,** and **Vehi, J.** Backstepping control of nonlinear building structures with hysteretic and frictional dynamics. European Control Conference, Kos, Greece, 2007.
38 **Zapateiro, M., Villamizar, R.,** and **Luo, N.** Semi-active seismic vibration control of structures equipped with magnetorheological dampers. *Int. J. Fact. Autom., Robot. Soft Comput.*, 2008, (1), 77–84.
39 **Kim, H.** and **Roschke, P.** Fuzzy control of base-isolation system using multiobjective genetic algorithm. *Comput.-Aid. Civil Infrastruct. Engng*, 2006, **21**, 436–446.
40 **Schurter, K.** and **Roschke, P.** Neuro-fuzzy control of structures using acceleration feedback. *Smart Mater. Struct.*, 2001, **10**, 770–779.
41 **Zapateiro, M., Luo, N., Karimi, H. R.,** and **Vehí, J.** Vibration control of a class of semiactive suspension system using neural network and backstepping techniques. *Mech. Syst. Signal Process.*, 2009, **23**(6), 1946–1953.
42 **Shield, C. K., French, C. W.,** and **Timm, J.** Development and implementation of the effective

force testing method for seismic simulation of large-scale structures. *Philos. Trans. R. Soc.*, 2001, **359**, 1911–1929.
43 **Mosqueda, G., Stojadinovic, B.,** and **Mahin, S.** Implementation and accuracy of continuous hybrid simulation with geographically distributed substructures, technical report, Earthquake Engineering Research Center, University of California, Berkeley, 2005.
44 **Jung, R. Y.** and **Shing, P. B.** Performance evaluation of a real-time pseudodynamic test system. *Eartha. Engng Struct. Dyn.*, 2006, **35**, 789–810.
45 **Carrion, J.** and **Spencer, B.** Model-based strategies for real-time hybrid testing, technical report, University of Illinois at Urbana-Champaign, 2007.
46 **Wang, Z., Yang, F., Ho, D. W. C.,** and **Liu, X.** Robust H_∞ control for networked systems with random packet losses. *IEEE Trans. Syst. Man Cybern., Part B: Cybern.*, 2007, **37**(4), 916–924.
47 **Limebeer, D. J. N., Anderson, B. D. O.,** and **Hendel, B.** A Nash game approach to mixed H_2/H_∞ control. *IEEE Trans. Automat. Control*, 1994, **39**, 69–82.
48 **Lin, W.** Mixed H_2/H_∞ control of nonlinear systems. In Proceedings of the 34th Conference on *Decision and control*, New Orleans, USA, 13–15 December 1995, pp. 333–338.
49 **Chen, X.** and **Zhou, K.** Multiobjective H_2/H_∞ control design. *SIAM J. Control Optim.*, 2001, **40**, 628–660.
50 **Chen, B. S.** and **Zhang, W.** Stochastic H_2/H_∞ control with state-dependent noise. *IEEE Trans. Autom. Control*, 2004, **49**(1), 45–57.
51 **Zhang, W., Zhang, H.,** and **Chen, B. S.** Stochastic H_2/H_∞ control with (x,u,v)-dependent noise: finite horizon case. *Automatica*, 2006, **42**(11), 1891–1898.
52 **Zhang, W., Huang, Y.,** and **Zhang, H.** Stochastic H_2/H_∞ control for discrete-time systems with state and disturbance dependent noise. *Automatica*, 2007, **43**(3), 513–521.
53 **Dahleh, M. A.** and **Pearson Jr, J. B.** L_1-optimal feedback controllers for MIMO discrete-time systems. *IEEE Trans. Autom. Control*, 1987, **32**, 314–322.
54 **Gahinet, P., Nemirovsky, A., Laub, A. J.,** and **Chilali, M.** *LMI control toolbox: for use with Matlab*, 1995 (The MATH Works, Inc., Natik, Massachusetts).
55 **Ho, D. W. C.** and **Lu, G.** Robust stabilization for a class of discrete-time nonlinear systems via output feedback: the unified LMI approach. *Int. J. Control*, 2003, **76**(2), 105–115.

APPENDIX

Lemma 1 [**55**]

For a given $\mathbf{M} \in \Re^{p\times n}$ with rank$(\mathbf{M}) = p < n$, assume that $\mathbf{Z} \in \Re^{n\times n}$ is a symmetric matrix; then there exists a matrix $\hat{\mathbf{Z}} \in \Re^{p\times p}$ such that $\mathbf{MZ} = \hat{\mathbf{Z}}\mathbf{M}$ if and only if

$$\mathbf{Z} = \mathbf{V}\begin{bmatrix}\mathbf{Z}_1 & 0\\ 0 & \mathbf{Z}_2\end{bmatrix}\mathbf{V}^{\mathrm{T}}$$

$$\hat{\mathbf{Z}} = \mathbf{U}\hat{\mathbf{M}}\mathbf{Z}_1\hat{\mathbf{M}}^{-1}\mathbf{U}^{\mathrm{T}}$$

where $\mathbf{Z}_1 \in \Re^{p\times p}$, $\mathbf{Z}_2 \in \Re^{(n-p)\times(n-p)}$, and the singular value decomposition of the matrix $\mathbf{M}$ is represented as $\mathbf{M} = \mathbf{U}[\hat{\mathbf{M}} \;\; 0]\mathbf{V}^{\mathrm{T}}$ with the unitary matrices $\mathbf{U} \in \Re^{p\times p}$, $\mathbf{V} \in \Re^{n\times n}$, and a diagonal matrix $\hat{\mathbf{M}} \in \Re^{p\times p}$ with positive diagonal elements in decreasing order.